

# XPS Characterization of Surface Fluorinated Poly(4-Methyl-1-Pentene)

J. M. MOHR,<sup>1</sup> D. R. PAUL,<sup>1,\*</sup> Y. TARU,<sup>1,†</sup> T. E. MLSNA,<sup>2</sup> and R. J. LAGOW<sup>2</sup>

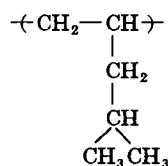
Departments of <sup>1</sup>Chemical Engineering and <sup>2</sup>Chemistry, Center for Polymer Research, The University of Texas at Austin, Austin, Texas 78712

## SYNOPSIS

The fluorinated surface layer of poly(4-methyl-1-pentene) membranes exposed to a dilute stream of fluorine gas has been characterized with X-ray photoelectron spectroscopy. The concentration and profile of reacted fluorine as a function of exposure time is determined. A computer routine was employed to deconvolute the poorly resolved carbon spectra after various fluorine exposure times. The concentrations of mono-, di-, and trifluorocarbon groups thus determined were used to propose specific structures of PMP at the surface after 1 and 15 min of fluorination. The carbon spectra collected at electron takeoff angles of 15°, 30°, and 90° were also deconvoluted, giving insight into the placement of fluorine as a function of depth. Oxygen is incorporated into the polymer during the fluorination reaction, and the O1s spectra was deconvoluted to determine how the oxygen is bound.

## INTRODUCTION

Gas-phase fluorination of solid polymers results in a thin layer of fluorinated material at the contacted surface. Surface fluorination has been used to improve liquid or vapor barrier characteristics<sup>1-4</sup> and the selectivity of gas separation membranes.<sup>5-11</sup> In this work, surface fluorination has been explored as a means for improving the gas separation properties of membranes based on poly(4-methyl-1-pentene) (PMP):



Its aliphatic hydrocarbon nature suggests that the primary reaction will be replacement of some of the hydrogen atoms with fluorine atoms. Other reactions

such as chain scission or cross-linking may follow. After the immediate surface is fluorinated, the reaction progresses deeper below the surface. Previous papers have reported the gas transport properties of the fluorinated PMP membranes and the thickness of the fluorinated layer as a function of fluorine exposure time.<sup>10,11</sup> The objective of this work was to learn more about the placement of fluorine atoms in the repeat unit by examining the fluorinated surface using X-ray photoelectron spectroscopy (XPS).

The fluorinated layer created by the process used has been shown to be relatively thin, typically no deeper than 1000 Å.<sup>3,5-8,11-13</sup> The surface sensitivity of XPS makes it particularly suited to probe this layer. XPS offers information at a number of levels, from a simple surface elemental composition to a detailed depth profile via angular dependent measurements. Both of these were used in this study. In addition, the poorly resolved carbon spectra were deconvoluted via a computer routine to give the concentrations of mono-, di-, and trifluorocarbon groups. Angular dependent studies were used to depth profile the fluorine composition in the top 90 Å of the membrane. The C1s spectra collected at electron takeoff angles of 15°, 30°, and 90° for selected fluorination times were also deconvoluted.

\* To whom correspondence should be addressed.

† Current address: Musashi Institute of Technology, 28-1 Tamazatsumi 1-chome, Setagaya-ku, Tokyo 158, Japan.

Journal of Applied Polymer Science, Vol. 42, 2509-2516 (1991)

© 1991 John Wiley & Sons, Inc.

CCC 0021-8995/91/092509-08\$04.00

## EXPERIMENTAL

Poly(4-methyl-1-pentene) (PMP) obtained from Scientific Polymer Products was solution-cast from cyclohexane onto a polysulfone-silicone rubber composite support membrane. The PMP layer had an average thickness between 1 and 2  $\mu\text{m}$  and was exposed to the fluorine/helium mixture for times varying from 1 to 15 min. Details of the membrane preparation and the fluorination procedures are discussed elsewhere in detail.<sup>10</sup>

The XPS spectra were obtained with a VG 1000 ESCA spectrometer using  $\text{MgK}\alpha$  exciting radiation (1253.6 eV). Typically, the X-ray gun was operated at 13 kV and 20 mA, and the sample chamber pressure was less than  $5 \times 10^{-9}$  torr. The gold  $4f_{7/2}$  level at 84 eV binding energy used for calibration had a full-width half-maximum (FWHM) of  $1.18 \pm 0.1$  eV.

Samples were mounted onto the sample probe with double-sided adhesive tape. Analysis times were kept short to minimize radiation damage to the sample.

Atomic sensitivity factor ratios were determined for fluorine to carbon and for oxygen to carbon from appropriate homogeneous polymer samples. The sensitivity factor is appropriate to the instrument on which the experiments are performed and is the product of several instrumental factors, namely, the photoionization cross section, the detection efficiency of the instrument, the efficiency of production from the photoelectron process, the angular efficiency factor, and the X-ray flux.<sup>14,15</sup> The ratio  $S_{\text{F}1s}/S_{\text{C}1s}$  was found to be 4.82 using poly(vinyl fluoride), 4.91 using poly(vinylidene fluoride), and 4.86 using poly(tetrafluoroethylene), giving an average value of 4.86. The ratio  $S_{\text{O}1s}/S_{\text{C}1s}$  was measured as 2.70 for poly(vinyl alcohol) and 2.75 for poly(methyl methacrylate), so an average value of 2.73 was used here. These homopolymers were obtained from the source indicated in parentheses: poly(vinyl fluoride) (DuPont), poly(vinylidene fluoride) (Pennwalt Corp.), poly(tetrafluoroethylene) (DuPont), poly(methyl methacrylate) (Rohm & Haas), and poly(vinyl alcohol) (Aldrich Chemical Co., 100% hydrolyzed).

Overlapping peaks of the C1s spectra were resolved into their individual component peaks with a computer routine. The deconvolution assumed a constant line width of 1.4 eV for each component peak. The individual component peak positions were determined from the literature and required an initial estimate of the intensity of each component

peak. The routine assumed all peaks were Gaussian in shape.

## RESULTS AND DISCUSSION

For the case of substrate material covered with a continuous overlayer of thickness  $d$ , the intensity of a core-level signal from the overlayer,  $I_i$ , is expressed as

$$I_i = I_{i,\infty} \left[ 1 - \exp\left(\frac{-d}{\lambda_i \sin \theta}\right) \right] \quad (1)$$

where  $I_{i,\infty}$  is the intensity arising from an infinitely thick layer of the overlayer,  $\lambda_i$  is the electron escape depth, and  $\theta$  is the electron emission angle relative to the plane of the sample surface.<sup>16-19</sup> When  $\theta$  is  $90^\circ$ , the depth from which the signal arises is governed only by the escape depth of the electrons. Equation (1) shows that when  $d/\lambda_i = 1, 2,$  and  $3$ ,  $I_i/I_{i,\infty} = 0.63, 0.87,$  and  $0.95$ , respectively, when  $\theta$  is  $90^\circ$ . Hence, to a reasonable approximation, the depth of material actually sampled is given by  $3\lambda_i$ . The escape depth  $\lambda_i$  depends on the material and on the kinetic energy of the electrons with values typically on the order of 5–30 Å for polymer materials.<sup>19-24</sup> Thus, in the XPS experiment, information

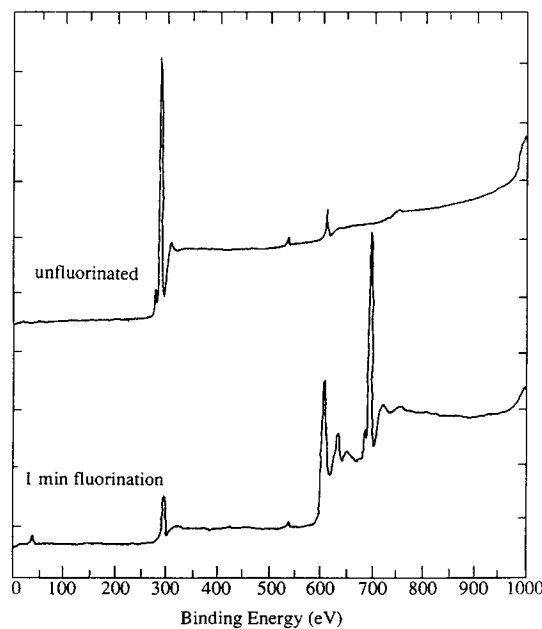


**Figure 1** XPS broad scan spectra of untreated PMP and after 1 min of fluorination.

is obtained from no more than about the top 90 Å of the sample.

Initial XPS measurements were done with the electron emission angle at 90° to determine the surface concentration within the maximum sampling depth. A broad scan spectra of PMP prior to fluorination and after 1 min of fluorine treatment is shown in Figure 1. The primary feature in the unfluorinated spectrum is the  $C_{1s}$  peak at 285 eV. A small oxygen peak at 532 eV is present, probably due to surface oxidation of the PMP. The spectrum of the fluorinated PMP has a less intense  $C_{1s}$  peak at 288 eV, an  $O_{1s}$  peak at 533 eV, and a  $F_{1s}$  peak at 690 eV. The small peak at 34 eV corresponds to the  $F_{2s}$  electron. Spectra were recorded for membranes after fluorination times of 1–15 min. The concentration of carbon, fluorine, and oxygen were determined from the spectra at each fluorination time, and the results are shown in Table I. The ratio of fluorine atoms to carbon atoms after 1 min of fluorination is 0.64, and this increases to 1.0 after 15 min of fluorine exposure or one-half of the hydrogen atoms in the PMP repeat unit have been replaced by fluorine atoms.

The  $C_{1s}$  peak from each spectra is shown in Figure 2. The carbon peak for unfluorinated PMP is narrow and well defined. Fluorination shifts the main  $C_{1s}$  peak to a slightly higher binding energy, and after 5 min of fluorination, this peak appears as a shoulder on a larger peak centered at ~ 286 eV. After fluorination, the overall  $C_{1s}$  peak consists of several partially resolved peaks that span ~ 10 eV. Deconvolution of the  $C_{1s}$  peaks can be accomplished by identifying the structural features that result from fluorination of PMP. Various studies have determined the binding energies of carbon–fluorine structures as a function of electronic environment.<sup>12,19,25–30</sup> Based on these studies, the binding

**Table I** Atomic Concentrations of Carbon, Fluorine, and Oxygen on a Hydrogen-Free Basis for PMP after Various Fluorine Exposure Times

Fluorination Time (min)	Atomic Concentration (%)			
	Carbon	Fluorine	Oxygen	F/C
1	59.0	37.9	3.1	0.64
2.5	54.7	42.4	2.8	0.77
5	51.0	46.5	2.5	0.91
7.5	51.2	46.4	2.4	0.91
12.5	49.8	47.7	2.5	0.96
15	49.0	49.0	2.0	1.00

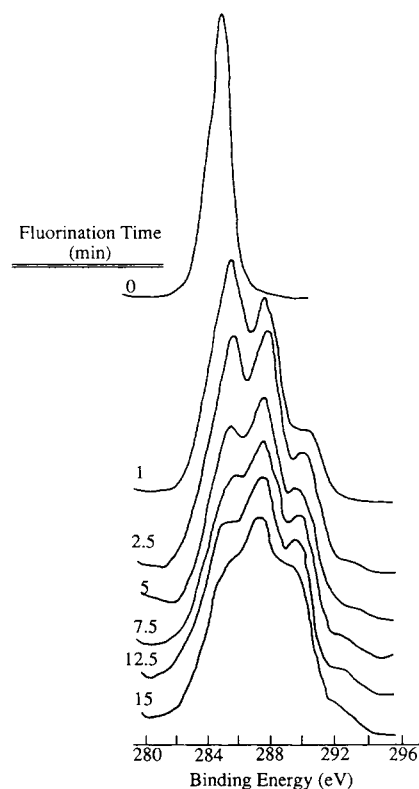


**Figure 2** Carbon peak of the XPS spectra of PMP after various fluorine exposure times.

energies of the structural features associated with fluorinated PMP were tabulated. The  $C_{1s}$  peaks were then resolved into nine component peaks, which represent envelopes containing a number of species of similar electron environment. The general structural feature of each component peak and the corresponding binding energy are listed in Table II.

Deconvolution of the  $C_{1s}$  spectra, illustrated in Figure 3 for PMP after 1 min of fluorination, was based on a constant line width of 1.4 eV for each component peak centered at the binding energies listed in Table II. The deconvolution gives the relative percentage of the nine component peaks after each fluorination time, and the results are summarized in Table III. At short fluorination times, the component peaks 1–4, which correspond to hydrocarbon and monofluorocarbon features, contribute most to the  $C_{1s}$  peak. As the fluorination time increases, the peaks associated with di- and trifluorocarbon features, peaks 7–9, begin to compose a larger fraction of the spectral area. The sum of the contributions of peaks 1, 2, and 3 represents the hydrocarbon environments; the sum of peaks 4, 5, and 6 represent the monofluorocarbon features; the

**Table II Representative Functional Groups for the Nine Component Peaks in the C1s Spectra of Fluorinated PMP and the Binding Energy Characteristic of Each Functional Group**

Peak	Representative Functional Group	Binding Energy (eV)	References
1	$\text{CH}_n$	285.0	25
2	$\text{CH}_n-\text{CF}$	$285.8 \pm 0.1$	25, 26
3	$\text{CF}-\text{CH}-\text{CF}$	$286.6 \pm 0.1$	12, 25, 26
4	$\text{CH}-\text{CHF}-\text{CH}$	$288.0 \pm 0.1$	12, 25
5	$\text{CHF}-\text{CF}-\text{CHF}$	$289.0 \pm 0.1$	12, 19, 27
6	$\text{CF}_2-\text{CF}-\text{CHF}$	$289.7 \pm 0.1$	19, 25
7	$\text{CH}-\text{CF}_2-\text{CH}$	$290.7 \pm 0.1$	12, 19, 26
8	$\text{CF}-\text{CF}_2-\text{CF}$	$291.7 \pm 0.1$	12, 25, 28
9	$\text{CF}_3$	$293.5 \pm 0.2$	25-27, 29-30

sum of peaks 7 and 8 denote the difluorocarbon groups; and peak 9 indicates trifluorocarbon features. These summations are tabulated in Table III and show the decreasing hydrocarbon content with fluorine exposure time. The increasing percentages of mono-, di-, and trifluorocarbon groups are shown in Figure 4. The monofluorocarbon concentration reaches a maximum at 43% after 2.5 min of fluorine exposure. The monofluorocarbon concentration remains constant while the concentration of di- and trifluorocarbon groups increases. The trifluorocar-

bon groups are not observed until 2.5 min of fluorine exposure.

The goodness of the deconvolution can be assessed by calculating the fluorine-to-carbon atomic ratio,  $F/C$ , from the fluorocarbon group concentrations

$$\frac{F}{C} = \frac{\%CF + 2 \cdot \%CF_2 + 3 \cdot \%CF_3}{100} \quad (2)$$

The fluorine-to-carbon atomic ratio calculated via eq. (2) should agree with the directly determined fluorine to carbon atomic ratios reported in Table I. The agreement is quite good, which is some evidence that the deconvolution was successful.

The information in Table I and Figure 4 can be used to propose specific structures of PMP after various times of fluorination. The ease of abstraction of hydrogen atoms from aliphatic hydrocarbons follows the order  $3^\circ > 2^\circ > 1^\circ$  (see Fig. 5).<sup>31,32</sup> Fluorine atoms are extremely reactive, and fluorination is by far the least selective halogenation process.<sup>31</sup> However, if the fluorine reaction with PMP were to follow conventional paths, then the  $3^\circ$  hydrogens in the PMP repeat unit would react first, followed by the  $2^\circ$  hydrogens, and the  $1^\circ$  hydrogens in the methyl groups would react last. After 1 min of fluorination, calculations based on the XPS results show on average 3.8 fluorine atoms and less than 1 oxygen atom per repeat unit. The remaining atoms are hydrogens that cannot be detected by XPS. The deconvolution results indicate the fluorine is distributed as follows: 3 CH, 2.3 CF, and 0.7 CF<sub>2</sub> groups. Structure I in Figure 5 meets the requirement of approximately four fluorine atoms distributed into two CF groups and one CF<sub>2</sub> group where the placement of the flu-

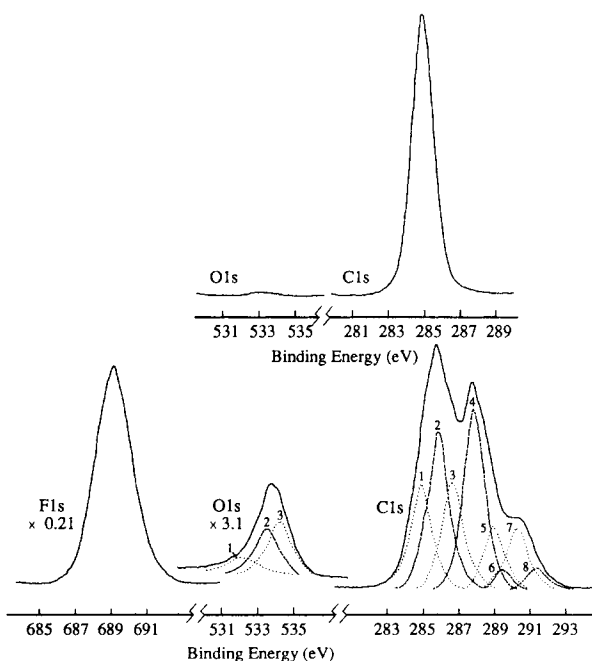


**Figure 3** C1s, O1s, and F1s spectra of unfluorinated PMP (above) and of PMP after 1 min of fluorine exposure with the O1s and C1s spectra deconvoluted.

**Table III** Component Peak Areas of the Deconvoluted C1s Spectra of Fluorinated PMP

Fluorination Time (min)	Component Peak Area (%)									% CH (1 + 2 + 3)	% CF (4 + 5 + 6)	% CF <sub>2</sub> (7 + 8)	% CF <sub>3</sub> (9)	F/C
	1	2	3	4	5	6	7	8	9					
1	12.9	13.5	23.2	22.6	13.2	3.1	8.7	2.8	0.0	49.6	38.9	11.5	0	0.60
2.5	9.2	9.2	19.7	21.5	18.5	3.0	12.2	5.5	1.0	38.1	43.0	17.7	1.0	0.80
5	8.3	8.3	17.5	24.5	15.1	3.4	15.1	6.0	1.6	34.1	43.0	21.1	1.6	0.88
7.5	7.4	6.8	16.9	23.6	15.2	4.7	16.9	6.4	2.0	31.1	43.5	23.3	2.0	0.95
12.5	6.2	6.0	16.8	22.4	15.1	5.7	18.4	6.7	2.6	28.8	43.2	25.1	2.6	1.01
15	5.8	5.6	16.0	21.7	14.0	7.2	19.3	7.2	3.0	27.4	42.9	26.5	3.0	1.04

orine atoms follows the conventional hydrocarbon reactivity. After 15 min of fluorination, there are six fluorine atoms and less than one oxygen atom with the fluorine distributed into 2.6 CF groups, 1.6 CF<sub>2</sub> groups, and 0.2 CF<sub>3</sub> groups. Structure II in Figure 5 fits the requirement of six fluorine atoms placed at the most reactive sites. However, the distribution of CF and CF<sub>2</sub> groups is equal rather than being 2.6 : 1.6. Structures III and IV have a more correct distribution of CF and CF<sub>2</sub> groups, but these structures require either five or seven fluorine atoms. Clearly, all of these structures can exist simultaneously to give an XPS spectral average of six fluorine atoms. The concentration of CF<sub>3</sub> groups is low with this group, occurring, on average, only one time for every five PMP repeat units. These structures are by no means definitive, but illustrate possible placement of the fluorine atoms.

The concentration of oxygen in the fluorinated PMP is relatively constant at approximately 2.5%,

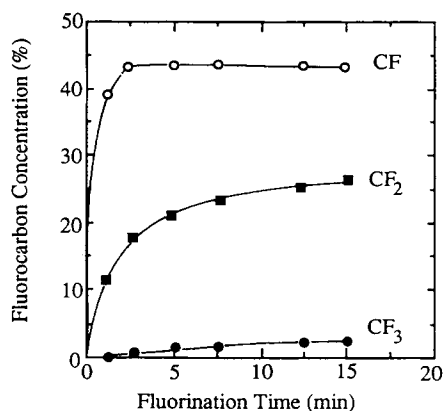


**Figure 4** Concentration of mono-, di-, and trifluorocarbon groups determined from deconvolution of the C1s spectra as a function of fluorination time. Content of unfluorinated carbon not shown but can be obtained by difference.

as shown in Table I, and corresponds to an average of 0.2 oxygen atoms per repeat unit. The most likely source of this is the low level of oxygen contamination present in commercially available fluorine gas. The oxygen may be present in the form of C—OH or C—O—C, which have binding energies of  $533.7 \pm 0.3$  eV,<sup>33,34</sup> in the form of carbonyl groups, C=O, centered at 532.7 eV,<sup>12,34</sup> or as water, which has an O<sub>1s</sub> binding energy of  $\sim 534.4$  eV.<sup>12</sup> The O<sub>1s</sub> spectra were deconvoluted as a function of fluorination time into these three component peaks as illustrated for the 1 min fluorinated PMP in Figure 3. Peak 1 corresponds to C=O groups, peak 2 corresponds to C—OH and C—O—C features, and peak 3 represents H<sub>2</sub>O. The results of the decon-

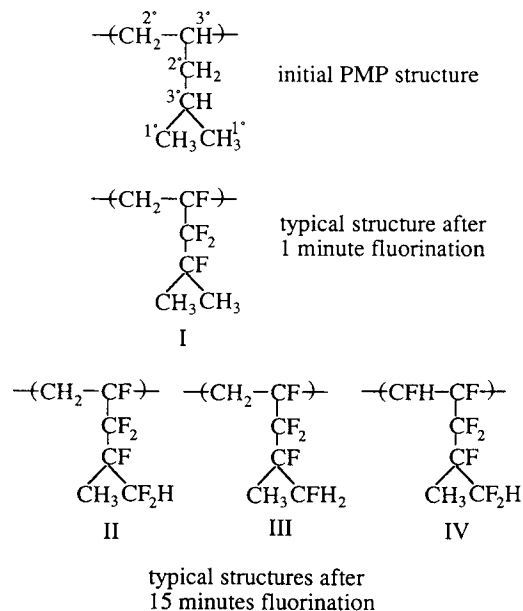


**Figure 5** PMP repeat unit and proposed placement of the fluorine atoms after 1 min and after 15 min of fluorination.

**Table IV** Component Peak Areas of the Deconvoluted O1s Spectra of Fluorinated PMP

Fluorination Time (min)	Component Peak Area (%)		
	Peak 1 (C=O)	Peak 2 (-COH, C-O-C)	Peak 3 (H <sub>2</sub> O)
1	14	40	46
2.5	21	33	46
5	24	38	38
7.5	25	31	42
12.5	33	33	33
15	36	29	34

volution, summarized in Table IV, show that at short fluorination times, the oxygen is present primarily in the form of water and C—OH or C—O—C features. At longer fluorination times, the amount of oxygen present in carbonyl groups increases until the oxygen is approximately evenly distributed among the three component peaks.

### ANGULAR DEPENDENT STUDIES

Up to this point, all the XPS measurements have been made by analyzing the photoelectron signal normal to the sample surface. With this experimental arrangement, the effective sampling depth is maximized. Figure 6 shows the relationships between the incident X-ray beam and the emitted photoelectrons, where  $\theta$ ,  $\lambda$ , and  $d$  are the takeoff angle of the emitted photoelectrons, the photoelectron escape depth, and the sampling depth, respectively. As discussed previously in relation to Eq. (1), the effective sampling depth is proportional to the product of escape depth and  $\sin \theta$ . The escape depth

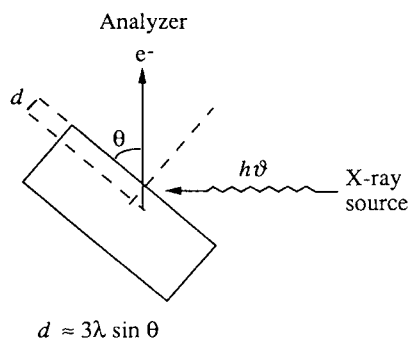


**Figure 6** Schematic representation of the relationship among the X-ray beam, the emitted photoelectrons, and the effective sampling depth as used in angular dependent studies.

is a function of the electron energy and the material, and it varies from  $\sim 5$  to  $\sim 30 \text{ \AA}$  in the 150–1500 eV range.<sup>18,20,22–24</sup> Therefore, the uppermost surface composition is emphasized by decreasing the electron takeoff angle.

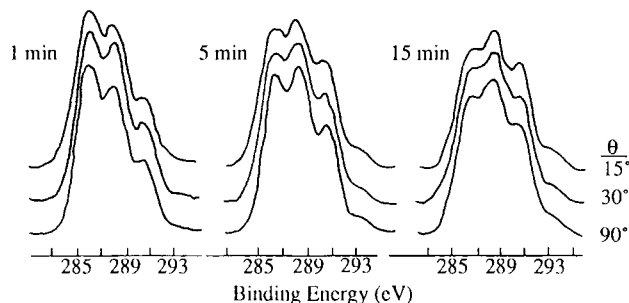


**Figure 7** C1s spectra of PMP after 1, 5, and 15 min of fluorination at electron takeoff angles,  $\theta$ , of 15°, 30°, and 90°.

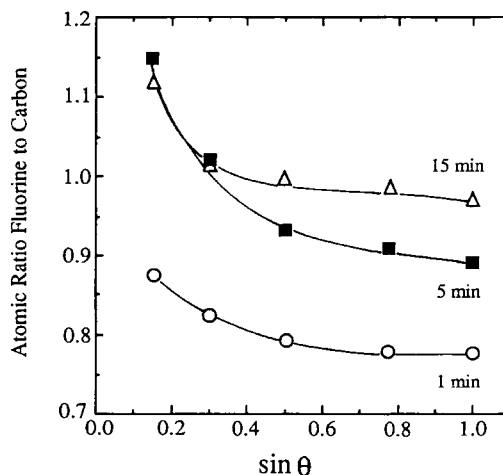


**Figure 8** Atomic ratio of fluorine to carbon as a function of electron takeoff angle for PMP after 1, 5, and 15 min of fluorination.

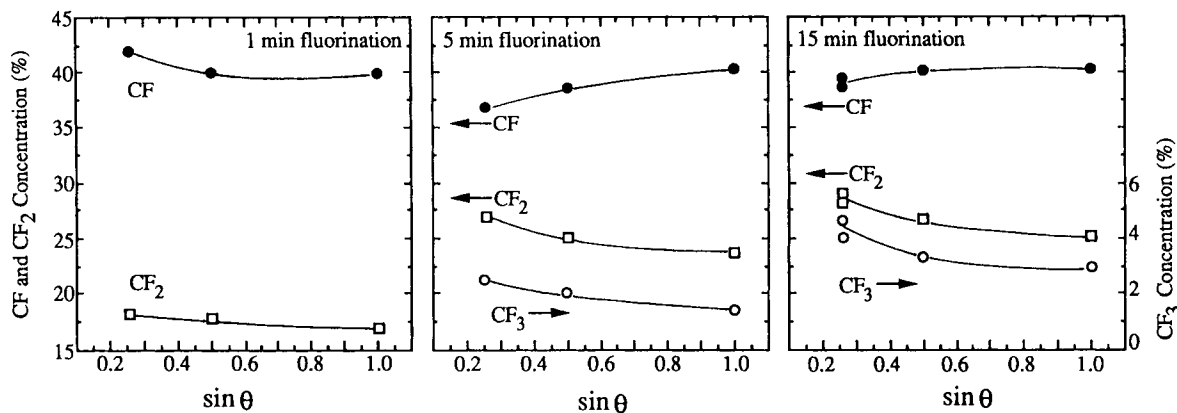


**Figure 9** Mono-, di-, and trifluorocarbon concentration determined from deconvolution of the  $C_{1s}$  spectra of 1, 5, and 15 min fluorinated PMP as a function of electron takeoff angle,  $\theta$ .

The  $C_{1s}$  spectra of PMP after 1, 5, and 15 min fluorine exposure at electron takeoff angles of  $15^\circ$ ,  $30^\circ$ , and  $90^\circ$  are shown in Figure 7. At  $15^\circ$ , the sampling depth is the most shallow at  $\sim 7.8 \text{ \AA}$  if  $\lambda = 20 \text{ \AA}$  and  $\sim 15.5 \text{ \AA}$  if  $\lambda = 30 \text{ \AA}$ . At this depth, the changing shape of the  $C_{1s}$  peak is very apparent, as the concentrations of mono-, di-, and trifluorocarbon groups increase with fluorination time. By 15 min of fluorination, the peaks centered at  $\sim 289 \text{ eV}$  and at  $\sim 291.5$ , associated with the di- and trifluorocarbon groups, are more prominent than is the hydrocarbon peak at  $\sim 285 \text{ eV}$ . The change in the  $C_{1s}$  peak at a given fluorination time with depth is also apparent. Figure 8 shows the fluorine to carbon atomic ratio against  $\sin \theta$  after 1, 5, and 15 min of fluorine exposure. There is some gradient of fluorine in the top  $90 \text{ \AA}$  of the polymer. The similarity in the 5 and 15 min curves up to  $\sin \theta = 0.3$  ( $18\text{--}27 \text{ \AA}$  for  $\lambda = 20\text{--}30 \text{ \AA}$ ) suggests that by 5 min of fluorination the immediate surface reaches a maximum level of fluorination and changes very little thereafter.

The  $C_{1s}$  peaks shown in Figure 7 were deconvoluted according to the procedure described above to determine the relative percentages of mono-, di-, and trifluorocarbon groups. Figure 9 shows the results of the deconvolution, giving the fluorocarbon concentration as a function of  $\sin \theta$  for the 1, 5, and 15 min fluorine exposure times. Trifluorocarbon groups are not present after 1 min of fluorination, and there is a shallow gradient in the monofluorocarbon groups. After 15 min of fluorination, di- and trifluorocarbon groups are present and the concentration of these groups changes within the sampling depth. This is as expected for a fluorine reaction front pro-

gressing into the surface that leaves the immediate surface more fluorinated than the inner surface.

## CONCLUSIONS

XPS was used to characterize the surface of PMP membranes after exposure to gaseous fluorine. A deconvolution procedure was employed to resolve the  $C_{1s}$  spectra giving the concentration of mono-, di-, and trifluorocarbon groups as a function of fluorine exposure time. With this information, specific structures of PMP fluorinated for 1 and 15 min are proposed. Angular dependent XPS shows a gradient of fluorine in the top  $\sim 90 \text{ \AA}$  of the membrane. Finally, the  $O_{1s}$  spectra was deconvoluted into three component peaks of carbonyl features,  $-\text{COH}$  and  $\text{C}-\text{O}-\text{C}$  groups, and water. Surface adsorption of water is a part of the  $O_{1s}$  spectra at all fluorination times, whereas the amount of carbonyl,  $-\text{COH}$ , and  $\text{C}-\text{O}-\text{C}$  features increase with fluorination time. Considering the high-vacuum environment in which the XPS analysis is done, one has to wonder why water is not rapidly desorbed. However, others have noted the presence of water in XPS analyses for other materials<sup>35</sup> and for some polymers.<sup>12</sup>

This material is based in part upon work supported by the Texas Advanced Technology Program under Grant No. 1607 and by the Separations Research Program at the University of Texas at Austin.

## REFERENCES

1. J. L. Scotland, U.S. Pat. 3,647,613 (March 7, 1972), assigned to British Resin Products Limited, London, England.

2. S. P. Joffe, U.S. Patent 2,811,468 (October 29, 1957), assigned to Shulton Inc., Clifton, N.J.
3. J. F. Gentilcore, M. A. Triallo, and A. J. Waytek, *Plast. Eng.*, **34**(9), 40 (1978).
4. K. A. Goebel, V. F. Janas, and A. J. Woytek, *Polym. News*, **8**, 37 (1982).
5. W. J. Koros, V. T. Stannett, and H. B. Hopfenberg, *Polym. Eng. Sci.*, **22**(12), 738 (1982).
6. C. L. Kiplinger, D. F. Persico, R. J. Lagow, and D. R. Paul, *J. Appl. Polym. Sci.*, **31**, 2617 (1986).
7. M. Langsam, M. Anand, and E. J. Karwacki, *Gas Sep. Purification*, **2**, 162 (1988).
8. M. Langsam, U.S. Pat. 4,657,564 (April 14, 1987), assigned to Air Products and Chemicals, Inc., Allentown, PA.
9. M. Langsam and A. C. L. Savoca, U.S. Pat. 4,759,776 (July 26, 1988), assigned to Air Products and Chemicals, Inc., Allentown, PA.
10. J. M. Mohr, D. R. Paul, T. E. Mlsna, and R. J. Lagow, to appear.
11. J. M. Mohr, D. R. Paul, Y. Taru, T. E. Mlsna, and R. J. Lagow, to appear.
12. D. T. Clark, W. J. Feast, W. K. R. Musgrave, and I. Ritchie, *J. Polym. Sci. Polym. Chem. Ed.*, **13**, 857 (1975).
13. C. S. Blackwell, P. J. Degen, and F. D. Osterholtz, *Appl. Spectrosc.*, **32**(5), 480 (1978).
14. C. D. Wagner, L. E. Davis, M. V. Zeller, J. A. Taylor, R. H. Raymond, and L. H. Gale, *Surf. Interface Anal.*, **3**(5), 211 (1981).
15. C. S. Fadley, R. J. Baird, W. Siekhaus, T. Novakov, and S. A. L. Bergstrom, *J. Electron Spectrosc. Relat. Phenom.*, **4**, 93 (1974).
16. D. Briggs, in *Handbook of X-Ray and Ultraviolet Photoelectron Spectroscopy*, D. Briggs, Ed., Heyden, London, 1978, Chap. 4.
17. J. C. Riviere, in *Practical Surface Analysis by Auger and X-Ray Photoelectron Spectroscopy*, D. Briggs and M. P. Seah, Eds., John Wiley, New York, 1983, Chap. 2.
18. D. T. Clark, *Adv. Polym. Sci.*, **24**, 125 (1977).
19. D. T. Clark and W. J. Feast, *J. Macromol. Sci. Rev. Macromol. Chem.*, **C12**(2), 191 (1975).
20. M. P. Seah and W. A. Dench, *Surf. Interface Anal.*, **1**, 2 (1979).
21. D. T. Clark and H. R. Thomas, *J. Polym. Sci. Polym. Chem. Ed.*, **15**, 2843 (1977).
22. M. Pijolat and G. Hollinger, *Surf. Sci.*, **105**, 114 (1981).
23. R. F. Roberts, D. L. Allara, C. A. Pryde, D. N. E. Buchanan, and N. D. Hobbins, *Surf. Interface Anal.*, **2**, 5 (1980).
24. D. R. Penn, *J. Electron Spectrosc. Relat. Phenom.*, **9**, 29 (1976).
25. D. T. Clark, W. J. Feast, D. Kilcast, and W. K. R. Musgrave, *J. Polym. Sci. Polym. Chem. Ed.*, **11**, 389 (1973).
26. D. T. Clark and D. Shuttleworth, *J. Polym. Sci. Polym. Chem. Ed.*, **16**, 1093 (1978).
27. D. T. Clark and D. Shuttleworth, *J. Polym. Sci. Polym. Chem. Ed.*, **18**, 27 (1980).
28. D. T. Clark and M. Z. Abraham, *J. Polym. Sci. Polym. Chem. Ed.*, **19**, 2129 (1981).
29. D. T. Clark and D. Shuttleworth, *J. Polym. Sci. Polym. Chem. Ed.*, **17**, 1317 (1979).
30. D. T. Clark and D. Shuttleworth, *J. Polym. Sci. Polym. Chem. Ed.*, **18**, 407 (1980).
31. J. M. Tedder, *Q. Rev.*, **14**, 336 (1960).
32. R. T. Morrison and R. N. Boyd, *Organic Chemistry*, 4th Ed., Allyn and Bacon, Boston, MA, 1983, p. 108.
33. H. R. Thomas and J. J. O'Malley, *Macromolecules*, **12**(2), 323 (1979).
34. D. T. Clark and H. R. Thomas, *J. Polym. Sci. Polym. Chem. Ed.*, **14**, 1671 (1976).
35. N. S. McIntyre in *Practical Surface Analysis by Auger and X-Ray Photoelectron Spectroscopy*, D. Briggs and M. P. Seah, Eds., John Wiley, New York, 1983, Chap. 10.

Received July 6, 1990

Accepted August 13, 1990